Astrophysical Masers:
Unlocking the Mysteries of the Universe
Proceedings IAU Symposium No. 336, 2017
A. Tarchi, M.J. Reid & P. Castangia, eds.

doi:10.1017/S1743921317010110

Eight new astrometry results of 6.7 GHz CH_3OH and 22 GHz H_2O masers in the Perseus arm

Nobuyuki Sakai, BeSSeL and VERA projects members

Mizusawa VLBI Observatory, National Astronomical Observatory of Japan,
2-21-1 Osawa, Mitaka, Tokyo 181-8588, Japan
email: nobuyuki.sakai@nao.ac.jp

Abstract. We report astrometric results for seven 6.7 GHz CH_3OH and one 22 GHz H_2O masers in the Perseus arm with VLBA and VERA observations. Among the eight sources, we succeeded in obtaining trigonometric parallaxes for all sources, except G098.03+1.44 at 6.7 GHz band. By combining our results with previous astrometry results (Choi *et al.* 2014), we determined an arm width of 0.41 kpc and a pitch angle of 8.2 ± 2.5 deg for the Perseus arm. By using a large sample of the Perseus arm (26 sources), we examined the three-dimensional, non-circular motions (defined as U, V and W) of sources in the Perseus arm as a function of the distance (D) perpendicular to the arm. Interestingly, we found a weighted mean of $< U > = 12.7 \pm 1.2$ km s^{-1} for 14 sources with $D < 0$ kpc (i.e. sources on the interior side of the arm) and $< U > = -0.3 \pm 1.5$ km s^{-1} for 12 sources with $D > 0$ kpc (i.e. sources exterior to the arm). These findings might be the first observational indication of the "damping phase of a spiral arm" suggested by the non-steady spiral arm model of Baba *et al.* (2013). The small pitch angle of the Perseus arm (< 10 deg) also supports the damping phase, based on "pitch angle vs. arm amplitude" relation shown in Grøsbol *et al.* (2004).

Keywords. Galaxy: kinematics and dynamics, ISM: clouds, masers, astrometry.

1. Introduction

Two formation mechanisms for spiral arms have been discussed in the literature:
(1) *the spiral structure rotates nearly uniformly although the material* (*star and gas*) *rotate differentially*, *or*
(*2*) *the arms are short − lived and reform as open structures*
(Goldreich & Lynden-Bell 1965). Mechanism (1) is known as the density-wave theory (Lin & Shu 1964), while mechanism (2) has often appeared in N-body simulations (e.g. Fujii *et al.* 2011). Measuring 3D velocity fields could potentialy descriminate between these mechanisms, but this is exceedingly difficult to do for external galaxies. In the Milky Way, however, VLBI astrometry studies have allowed us to measure precise distances and 3D velocity fields toward star-forming regions (SFRs) associated with spiral arms (Reid & Honma 2014b). Sakai *et al.* (2012) showed systematic inward motion and slow rotation in the Perseus arm with seven astrometric results and Choi *et al.* (2014) confirmed the same systematic motion, increasing the results to 25 sources.

TGAS in *Gaia* DR1 (with 2.5 million stellar astrometry results) was released in September, 2016, with limited accuracy (systematic error of 0.3 mas)†, but forthcoming catalogs (*Gaia* DR 2 and following) will allow us to study spiral arms beyond several kpc from the Sun including the Perseus arm. We will have precise gas (SFRs) and stellar astrometric data within few years and be able to discriminate between the two mechanisms

† https://gaia.esac.esa.int/documentation/GDR1/pdf/GaiaDR1_documentation_1.1.pdf

discussed above. In other words, we will be able to answer the question "Are spiral arms quasi stationary (like density-waves) or non-stationary (dynamic) structures?" based on observational data.

Here, we report eight new astrometric results from the VLBA and VERA, which better reveal the structure and kinematics of the Perseus arm. Based on the results, we discuss which mechanism (quasi stationary or non-stationary model) is consistent with the data.

2. Observations & Data reduction

We observed 13 CH_3OH ($J_K = 5_1 - 6_0 A^+$) masers, with rest frequency of 6.668519 GHz, under VLBA programs BR149R, S, T and U†. The observation results for seven of these sources are presented here. A more detailed explanation of the observations will be provided in a forthcoming paper (Sakai *et al.* 2017 in preparation). We also observed two H_2O ($J_{K_{-1}K_1} = 6_{16} - 5_{23}$) masers, with rest frequency of 22.235080 GHz with VERA, and we report results here for one of the source. Based on CO $l-v$ emission (Dame *et al.* 2001), the eight sources associated with the Perseus arm.

The VLBA data reduction was done with the NRAO Astronomical Image Processing System (AIPS) and a Parsel tongue script used in previous BeSSeL Survey papers (e.g., Xu *et al.* 2016). Details of the fitting of parallax and proper motion for 6.7 GHz CH_3OH data are described in Reid *et al.* (2017). For the VERA data, AIPS was also used, and the details of the data reduction are summarized in Sakai *et al.* (2015).

3. Results & Discussion

We obtained trigonometric parallaxes and proper motions for seven sources, except for G098.03+1.44. Since G098.03+1.44 was faint and extended, we could not obtain a reliable parallax result. Our results and previous ones obtained from Choi *et al.* (2014) are superposed in a face-on view of the Milky Way in Figure 1.

3.1. *Pitch angle and arm width of the Perseus arm*

We fitted a logarithmic spiral arm model to the locations of the Perseus arm sources using the following equation:

$$\ln(R/R_{\rm ref}) = -(\beta - \beta_{\rm ref})\tan\psi, \tag{3.1}$$

where $R_{\rm ref}$ and $\beta_{\rm ref}$ are a reference Galactocentric distance and azimuth for the arm. β is defined as zero degrees toward the Sun as viewed from the Galactic center and increases with Galactic longitude, and ψ is the pitch angle of the arm.

We obtained $R_{\rm ref} = 9.97 \pm 0.15$ kpc, $\beta_{\rm ref} = 13.7$ deg and $\psi = 8.3 \pm 2.5$ deg for the Perseus arm. The results are consistent with those in Reid *et al.* (2014a) within errors. In the fitting, we assumed an arm width 0.43 kpc for the Perseus arm (Reid *et al.* 2014a). Figure 1 shows the result of the fitting.

3.2. *Non-circular motion of the Perseus arm*

Next, we discuss non-circular motions in the Perseus arm derived from the astrometric results and LSR velocities, using a model of the rotation curve and peculiar solar motion ($U_\odot$, $V_\odot$, $W_\odot$). We assume the universal rotation curve (Persic *et al.* 1996) and ($U_\odot$, $V_\odot$, $W_\odot$) = (10.5 ± 1.7, 14.4 ± 6.8, 8.9 ± 0.9) km s^{-1} (Reid *et al.* 2014a). Black arrows in Fig. 1 show residuals (i.e., non-circular motions) to the model.

† Please see the BeSSeL project HP: `http://bessel.vlbi-astrometry.org/observations`

https://doi.org/10.1017/S1743921317010110 Published online by Cambridge University Press

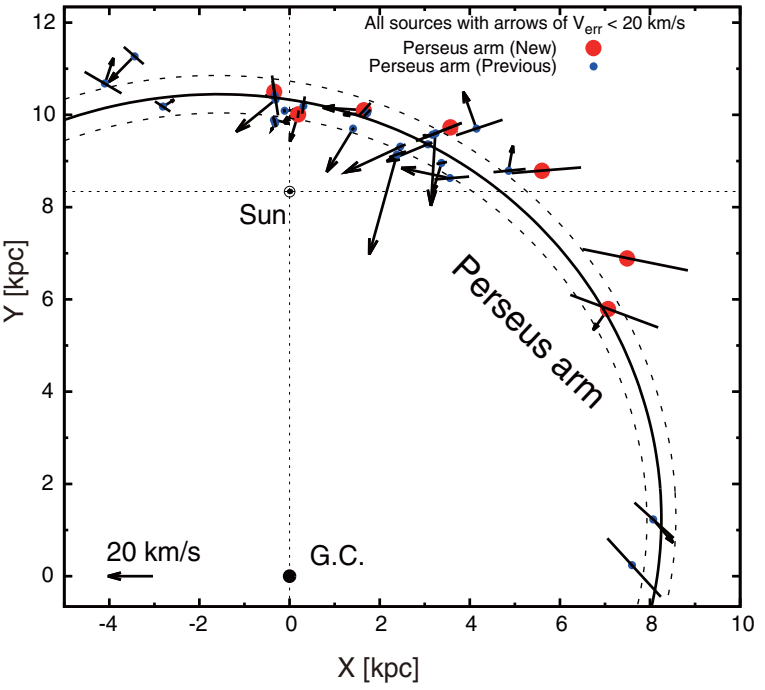

Figure 1. Spatial distribution and non-circular motions of the Perseus arm sources. Arrows indice non-circular motions only for sources with uncertainties less than 20 km s^{-1}. The scale of 20 km s^{-1} is shown at the lower left of the image. The Sun is located at (X, Y) = (0, 8.34) kpc. The universal rotation curve (Persic *et al.* 1996) and ($U_\odot$, $V_\odot$, $W_\odot$) = (10.5 ± 1.7, 14.4 ± 6.8, 8.9 ± 0.9) km s^{-1} (Reid *et al.* 2014a) are assumed.

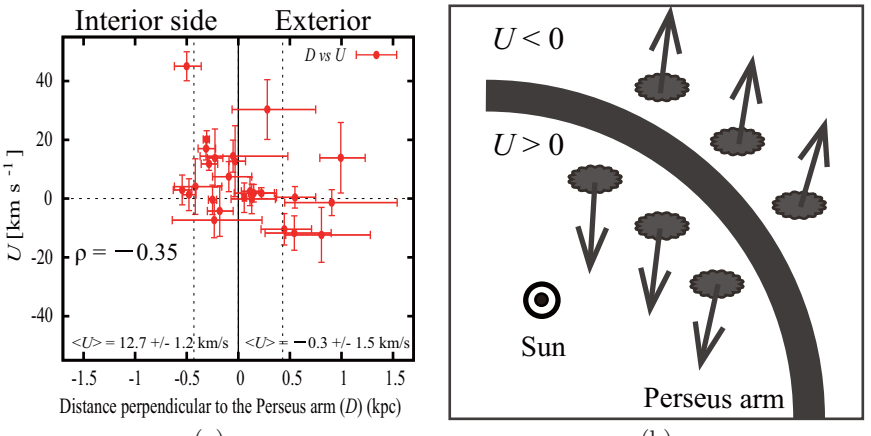

(a) (b)

Figure 2. (a) The U component of Non-circular motion as a function of distance perpendicular to the Perseus arm (D). $D < 0$ corresponds to the interior side of the Perseus arm (i.e. closer to the Sun from the center of the arm) while $D > 0$ indicates exterior to the Perseus arm. The symbol <> denoted in each side of the figure shows weighted mean of the non-circular motion while the value ρ superposed on the figure represents the correlation coefficient. Solid line on the figure shows the position of the Perseus arm while vertical dashed lines on the figure represent the arm width (= 0.43 kpc, see text). (b) Schematic view of the figure (a). Arrows on the figure show tendency of the non-circular motion of U seen in the Perseus arm.

https://doi.org/10.1017/S1743921317010110 Published online by Cambridge University Press

Figure 2a displays the non-circular motion toward the Galactic center (defined as U) as a function of distance perpendicular to the Perseus arm (D). The data hints at a negative slope with correlation coefficient of -0.35. This suggests that sources on the near side of the Perseus arm (sources with $D < 0$) are moving toward the Galactic center with a weighted mean of $< U > = 12.7 \pm 1.2$ km s^{-1}, while those on the far side (those with $D > 0$) are moving oppositely with $< U > = -0.3 \pm 1.5$ km s^{-1}. This tentative result, if confirmed, would be the first observational indication of the damping phase of the Perseus arm.

Baba *et al.* (2013) conducted three-dimensional N-body simulations to examine the characteristics of stellar spiral arms in disk galaxies. They found that a growing (high density) phase appeared with a large pitch angle >30 deg, and the spiral arm later showed a damping (low density) phase with the samller pitch angle (see Fig. 7 of Baba *et al.* 2013). Observationally, Grøsbol *et al.* (2004) examined structural parameters of 54 normal spiral galaxies and found (1) a typical range of pitch angles between 5-30 deg and (2) a proportional relation of *tan*(pitch angle) versus relative arm amplitude (see Fig. 8 of Grøsbol *et al.* 2004). If the Milky Way is a normal spiral galaxy, the Grøsbol *et al.* (2004) result suggests the Perseus arm is now in the damping (low density) phase.

We will be able to validate our conclusion regarding the damping phase of the Perseus arm) by adding stellar astrometric results from *Gaia* DR2 (released in April, 2018), which might allow us to obtain a more conclusive answer to a major problem of the Galactic astronomy.

We are grateful to BeSSeL and VERA projects members for the support they offered during observations. We are also grateful to Dr. Mark J. Reid for carefully reading and editing the manuscript. We would like to thank the LOC and SOC of IAUS 336 for organizing the productive conference in Sardegna, Italy.

References

Baba, J., Saitoh, T. R., & Wada, K. 2013, *ApJ*, 763, 46
Choi, Y., Hachisuka, K., Reid, M. J., Brunthaler, A., Menten, K. M., *et al.* 2014, *ApJ*, 790, 99
Dame, T. M., Hartmann, D., & Thaddeus, P. 2001, *ApJ*, 547, 792
Fujii, M., Baba, J., Saitoh, T. R., Makino, J., Kokubo, E., & Wada, K. 2011, *ApJ*, 730, 109
Goldreich, P.,& Lynden-Bell, D. 1965, *MNRAS*, 130, 125
Grøsbol, P., Patsis, P. A., & Pompei, E. 2004, *A&A*, 423, 849
Lin, C. C. & Shu, F. H. 1964, *ApJ*, 140, 646
Persic, M, Salucci, P. & Stel, F. 1996, *MNRAS*, 281, 27
Reid, M. J., Menten, K. M., Brunthaler, A., Zheng, X. W., *et al.* 2014a, *ApJ*, 783, 130
Reid, M. J. & Honma, M. 2014b, *ARA&A*, 52, 339
Reid, M. J., Brunthaler, A., Menten, K. M., Sanna, A., Xu, Y., Li, J. J., *et al.* 2017, *AJ*, 154, 63
Sakai, N., Honma, M., Nakanishi, H., Sakanoue, H., Kurayama, T., *et al.* 2012, *PASJ*, 64, 108
Sakai, N., Nakanishi, H., Matsuo, M., Koide, N., Tezuka, D., *et al.* 2015, *PASJ*, 67, 69
Xu, Y., Reid, M. J., Menten, K., Sakai, N., Li, J., Brunthaker, A., *et al.* 2016, *SciA*, 2, 9